2022

Design of a Direct-Contact Thermal Energy Storage Heat Exchanger for the NIST Net-Zero Residential Test Facility: Part 2 Heat Exchanger Design

Mark Kedzierski

Lingnan Lin

Design of a Direct-Contact Thermal Energy Storage Heat Exchanger for the NIST Net-Zero Residential Test Facility: Part 2 Heat Exchanger Design

Mark KEDZIERSKI*, Lingnan LIN

National Institute of Standards and Technology,
Gaithersburg, Maryland, USA
301-975-5282, mak@nist.gov

* Corresponding Author

ABSTRACT

This paper describes the second part of the design of a direct-contact heat exchanger (DCHEX) to be used for thermal energy storage in the Net-Zero Energy Residential Test Facility (NZERTF) at the National Institute of Standards and Technology (NIST). The heat exchanger was designed for heat exchange between a phase-change material (PCM) and refrigerant. The selection of a PCM that would be immiscible with the refrigerant and have a freezing point temperature of approximately of 285 K is covered in the Part 1 companion paper. Part 2 of the project presented here provides a design for direct-contact heat exchange between octanoic acid (continuous phase) and the dispersed phase R410A. Twin DCHEXs were designed to house a vertical column of PCM and to distribute the refrigerant flow throughout the PCM. The height of the PCM column was determined with measurements from the literature that were re-correlated to predict the droplet heat transfer coefficient and the required height of the PCM column. A disengagement section was designed to prevent entrainment of PCM droplets into the exiting refrigerant vapor during the PCM charging. Basic equations are provided so that the design may be modified for a different PCM mass, refrigerant flow rate, temperature difference and operating fluids. A schematic drawing of the DCHEX with placement of orifice holes, mist eliminator, and piping was given. The energy storage capacity of the DCHEX is approximately 191 MJ and has the potential of providing a 33 % energy savings in cooling the NZERTF.

1. INTRODUCTION

A proposed solution for improved energy management that incorporates a Phase Change Material (PCM) for Thermal Energy Storage (TES) into a residential air conditioner was modeled by Kedzierski et al. (2018). They showed that a non-conventional ASHP with improved efficiency during electrical peaks used 6 % to 33 % less energy than the conventional system. Some of this improvement is because the PCM provided all of the cooling needs during the peak times when air conditioning operational efficiency is low, and some improvement is due to the fact that the unit runs nearly continuously instead of cycling on and off to meet the load, thus, avoiding a typical 2 % to 8 % loss in efficiency due to cycling (Baxter and Moyers 1985). When the PCM provides all the cooling, the electricity requirements for air-conditioning are almost negligible. The efficiency increases because the PCM is frozen (energy is stored) when the system operates at its peak efficiency, i.e., while the outdoor temperature is low. The potential value of these savings based on electricity consumption are significant and would add to those from greater local use of PV and from using time-dependent electricity rates to consumers' advantage.

Kedzierski et al. (2018) demonstrated that the key to maximizing the efficiency of the PCM-TES ASHP was to minimize the thermal resistance between the PCM material and the refrigerant and the indoor air. It follows that the performance of TES with PCM can be dramatically improved by using direct-contact heat transfer. Direct-contact heat transfer with the PCM eliminates the heat transfer resistance associated with tube walls that typically separate the PCM from the heat transfer fluid. A direct-contact heat exchanger (DCHEX) involves a heat transfer fluid flowing through and in direct contact with an immiscible solid-liquid PCM (SL-PCM). The enhanced heat transfer facilitates and significantly improves the charging/discharging process due to reduced thermal resistances. The improved heat transfer efficiency also allows the use of SL-PCMs that have relatively low thermal conductivity but high latent heat, which improves the energy storage density. In addition, the size and weight of a DCHEX is appreciably smaller than

that of a conventional "indirect" heat exchanger due to the elimination of structures like tubes and fins, which also has the additional benefit of reduced capital, material and manufacturing costs. Because of the high energy storage density and the high heat transfer efficiency, along with the significant size and weight savings, PCM-DCHEX can facilitate light, compact, and high-performance thermal energy storage systems.

Although the structure of PCM-DCHEX is simpler than conventional heat exchangers, the heat transfer and fluid flow are more complex, and a temporal pressure drop prediction is not possible. Consequently, this report provides a preliminary design of a direct-contact PCM-TES DCHEX for the NZERTF air-conditioner based on heat transfer and not pressure drop. The DCHEX is sized for the required air-conditioning load of the NZERTF. The refrigerant nozzle was designed to provide a well distributed flow through the PCM. A PCM with low vapor pressure and that was immiscible with R134a (and presumably R410A) was identified. Kedzierski et al. (2014) identified a remote/discrete PCM design for PCM storage with a residential ASHP. The purpose of the present investigation is to design a DCHEX for discrete PCM energy storage for use in air conditioning NIST's NZERTF. Accordingly, this paper determines the salient design parameters for an efficient and viable thermal energy storage using phase-change materials in a heat pump for net-zero homes.

2. DIRECT-CONTACT HEAT EXCHANGER (DCHEX) DESIGN

The general design of the DCHEX for heat exchange between a refrigerant and an immiscible PCM for use as residential energy storage is shown in Figure 1. Liquid refrigerant flows in from the bottom of the DCHEX and up through the PCM to cool it. Conversely, when the refrigerant vapor is being cooled and condensed, the refrigerant flows downward through PCM after it enters from the top of the DCHEX and past the eliminator. The DCHEX is mainly a pressure tank with provisions to facilitate the distribution of the refrigerant flow through the PCM and to ensure that the PCM remains in the vessel. Both the 5-micron sieve placed over the lower distribution orifice plate and the upper tank screened eliminator and vapor-liquid disengagement section are designed to keep the PCM in the DCHEX. The effective diameter of the holes in the sieve (s) was calculated from the surface tension (σ_p) forces required to hold the mass of PCM in the column height L:

$$s \le \frac{4\sigma_p}{\rho_p g L} = 6.72\times10^{-6}\,\text{m} \tag{1}$$

The properties of octanoic acid (shown in Table 1 of Kedzierski and Lin, 2020) were used to evaluate Eq. (1). Here, the symbol for the PCM liquid density is ρ_p, and that for the gravitational acceleration is g. The orifice plate was designed with 127 evenly-spaced 0.25 mm diameter orifices to promote well distributed flow of refrigerant through the PCM. The orifice plate also provides structural support for the mass of PCM above it and seals at the edge of the plate where the plate and the tank meet. The orifice hole spacing is approximately 73 mm on the radius with the outermost ring of holes being approximately 17 mm from the edge of the plate and the first hole in the plate-center. In the PCM charging mode, the sieve will break the liquid refrigerant droplets rising from the orifice plate into micro-droplets, but due to their proximity, significant agglomeration is expected to occur.

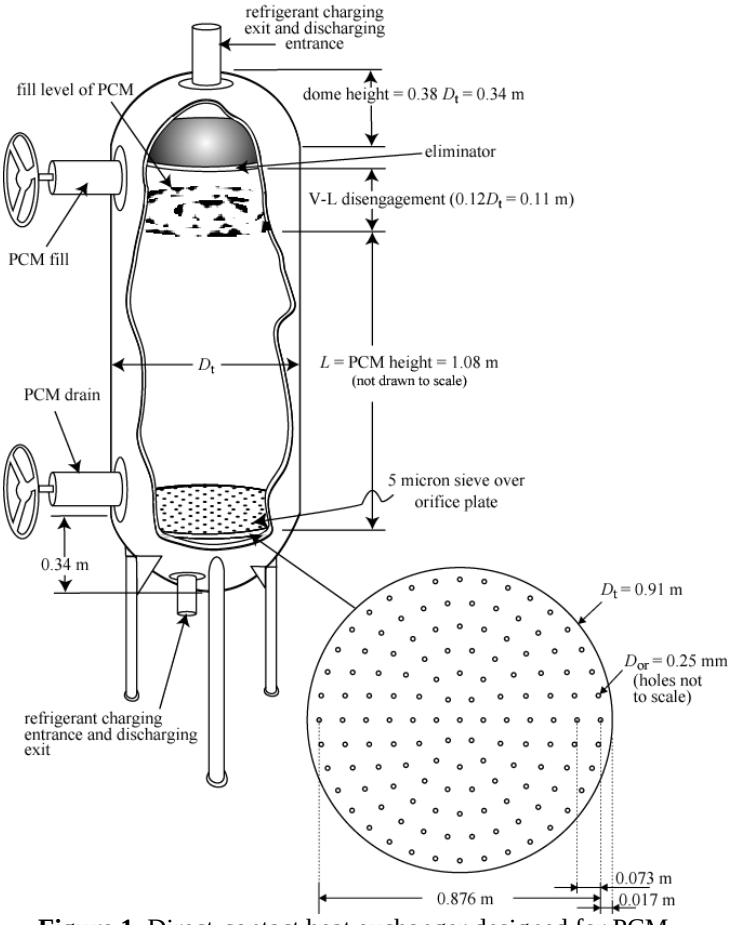

Figure 1 Direct-contact heat exchanger designed for PCM and refrigerant

Consequently, the heat transfer performance will be between that produced by the larger droplets of the orifice plate and the smaller droplets of the sieve. Because the amount of droplet agglomeration is not easily predicted (Deepu and Baus, 2014; Sideman and Gat, 1966), the DCHEX was designed based on the orifice-plate droplet size in order to ensure there is sufficient PCM height for complete refrigerant evaporation and condensation.

The tank is filled with PCM to a level of *L*, which is a key design parameter for the DCHEX. The height of the PCM is crucial because if the DCHEX is too tall, then it will not fit between the floor and ceiling of a typical residential basement; if it is too short, then the droplets will not completely evaporate as they rise to the upper surface of the PCM. The total mass of octanoic acid as the PCM is approximately 1285 kg, giving a storage capacity of approximately 191 MJ, which is roughly 5 % larger than the required energy storage capacity of the NZERTF (Kedzierski et al., 2018). This mass fixes the PCM volume, which fixes the diameter of the tank once its height is chosen. Preliminary calculations showed that in order to keep the tank height less than the basement ceiling and the tank thickness as required by a pressure vessel within reason, the mass of PCM was split into two DCHEXs.

In the droplet evaporation mode, only saturated refrigerant vapor should exit the top of the DCHEX. Consequently, the DCHEX design should guard against the potential entrainment of the PCM into exiting refrigerant vapor. Droplet entrainment occurs when the forces that lift a droplet into the entraining flow are larger than those forces that act on it in the opposite direction of the flow. Clift et al. (1978) presented an analysis of the seven different forces on a droplet. The present analysis only considers the buoyant force ($F_b = \rho_{rv} D_p^3 g\pi / 6$) and the drag force ($F_d = C_d \rho_{rv} D_p^2 u_{rv}^2 \pi / 8$) that act to entrain the droplet and the gravity force ($F_g = \rho_p D_p^3 g\pi / 6$) that acts to keep the PCM with its bulk mass. The velocity of the refrigerant vapor above the PCM is u_{rv}. If the ratio of the sum of the buoyance and drag force to the gravity force is sufficiently less than 1, then it is likely that droplet entrainment will not occur. This ratio can be expressed in terms of fluid properties while using the expressions for the various forces that are given by Clift et al. (1978):

$$\frac{F_b + F_d}{F_g} = \frac{\rho_{rv}}{\rho_p} + \frac{12 C_d \dot{m}_r^2}{\pi^2 D_p D_t^4 \rho_p \rho_{rv} g} < 1 \tag{2}$$

The density of the refrigerant vapor above the PCM and its total mass flowrate are ρ_{rv} and $\dot{m}_r$, respectively. The drag coefficient (C_d) for spherical particles was taken from Clift et al. (1978):

$$C_d = \frac{24}{\mathrm{Re}_p}\left[1 + 0.1315\,\mathrm{Re}_p^{0.82 - 0.05\ln(\mathrm{Re}_p)}\right] \tag{3}$$

The Reynolds number for the PCM particle (Re_p) was calculated as:

$$\mathrm{Re}_p = \frac{4\dot{m}_r D_p}{\pi \mu_{rv} D_t^2} \tag{4}$$

where μ_{rv} is the dynamic viscosity of the refrigerant vapor. The values of Re_p were between 1.2 and 2.5, which is within the range that Eq. (3) is valid.

Figure 2 plots Eq. (2) as a function of the PCM particle diameter (D_p). Figure 2 was made while using a PCM heat exchanger tank (D_t) diameter of 0.91 m and a refrigerant flow rate of 0.018 kg·s^{-1}, which is half the expected flow rate of the NZERTF ASHP (Kedzierski et al., 2018). Figure 2 shows that, for PCM droplets with diameters between 0.3 mm and 0.6 mm, the lifting forces on the droplet are always less than 5 % of the gravity force. Consequently, PCM droplet entrainment should not occur for the given refrigerant mass flowrate and PCM tank diameter. A simple estimate for the minimum vapor-liquid disengagement height (H_D) to reduce droplet entrainment when it is expected to occur and when an eliminator is not used is given by GPSA (2004):

$$H_D = \frac{u_{rv}}{u_T} D_t \tag{5}$$

Equating the F_g to the sum of F_b and F_d, and solving for the droplet velocity yields the terminal velocity of the droplet (u_T):

$$u_T = \sqrt{\frac{4(\rho_p - \rho_{rv}) D_p g}{3 C_d \rho_{rv}}} \tag{6}$$

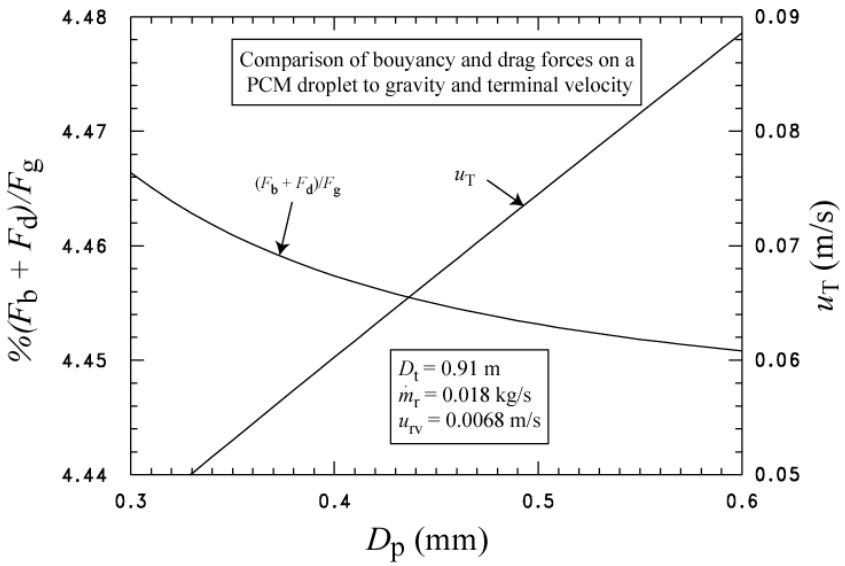

Figure 2 Comparison of measured buoyancy and drag forces on a PCM droplet to gravity as a function of droplet size and terminal velocity

Although Eq. (5) is conveniently simple, the origin of its derivation is not easily discerned. The u_T is the maximum velocity that a PCM droplet would obtain if it were to be dropped into an atmosphere of refrigerant vapor and allowed to fall long enough to achieve zero acceleration. It is not obvious why Eq. (5) gives one diameter for H_D when the vapor velocity is just large enough to keep a droplet from falling. Nevertheless, Eq. (5) is an accepted methodology of GPSA (2004) and Eq. (5) predicts a small H_D (as shown below), which is consistent with the lift forces on the droplet being less than 5 % of the gravity force.

Figure 2 plots u_T as a function of potential droplet sizes. For fixed value of u_{rv} (0.0068 m/s), the u_{rv}/u_T varies between roughly 0.008 and 0.015. According to Eq. (5), this corresponds to an H_D roughly between 7 mm and 14 mm. Figure 1 shows that the dome height of the semi-spherical end of the tank is approximately $0.38D_t$ or 0.34 m, which exceeds the GPSA (2004) recommended H_D in Eq. (5) by at least 0.32 m. Although the dome provides a sufficient H_D, an additional disengagement height of $0.12D_t$ (0.11 m) was added directly above the PCM surface to provide space between the PCM and the eliminator. Combining the two heights gives the space above and below the screen eliminator as $0.5D_t$. Together, the screen eliminator and the disengagement height of $0.5D_t$ ensures that no entrainment of PCM in the refrigerant vapor flow is likely to occur. Considering the height necessary for the above components, the entrance and exit ports and supporting legs, the allowable height for the PCM column is less than 1.2 m.

The DCHEX was designed based on the refrigerant evaporation mode because the refrigerant evaporation mode will have a similar, but a slightly larger, required PCM column height than the refrigerant condensation mode for complete phase change. The heat transfer between a droplet rising and evaporating within a column of liquid needs to be quantified to calculate the PCM column height for complete evaporation. Smith et al. (1982) determined a droplet heat transfer coefficient (h_d) from an explicit solution for evaporating droplets rising through a stagnant continuous phase. The droplet heat transfer coefficient was expressed in terms of a droplet Nusselt number (Nu_d) with the traditional relationship between heat and mass transfer (Incropera and DeWitt, 2002):

$$Nu_d = \frac{h_d D_d}{k_c} = \gamma \, Re_c^x \, Pr_c^{1/3} \tag{7}$$

Here D_d is the diameter of the dispersed phase droplet, which increases by producing vapor as it rises through the continuous phase from the all-liquid D_{do} at the orifice plate exit to the all-vapor diameter $D_{do}(\rho_{dl}/\rho_{dv})^{1/3}$ at the top of the PCM column. The expression for the all-vapor diameter assumes that agglomeration with other droplet/bubbles does not occur. The ρ_{dl} and the ρ_{dv} are the liquid and vapor densities of the dispersed phase, respectively. In their experiment, Smith et al. (1982) used 0.5 mm diameter orifice holes that produced an initial droplet diameter (D_{do}) of 1.0 mm. They verified the value of D_{do} with photographic observations. The present orifice plate design uses 0.25 mm diameter orifices and, following what was observed by Smith et al. (1982), assumes that the D_{do} is twice that value, i.e., 0.5 mm. The k_c, the Re_c, and the Pr_c are the thermal conductivity, the Reynolds number, and the Prandtl number of the continuous phase, respectively.

Smith et al. (1982) included Eq. (7) as part of an explicit derivation for the required height of continuous phase liquid (L) to just completely evaporate rising droplets from saturated liquid to saturated vapor for a given superheat (ΔT). The superheat was defined as the temperature difference between the saturated dispersed phase and the uniform temperature of the stagnate continuous phase. The Smith et al. (1982) expression for L and ΔT is based on properties of the dispersed and continuous phases:

$$\left(\frac{\rho_{dl}}{\rho_{dv}}\right)^{\frac{2-x}{3}} - 1 = 2\left(\frac{\rho_c k_c}{\rho_{dv}\mu_c \lambda_d D_{do}}\right)(2-x)\gamma\, \mathrm{Re}_{co}^{x-1}\, \mathrm{Pr}_c^{1/3}\, L\Delta T \tag{8}$$

where ρ_c, μ_c, λ_d, are the liquid density and viscosity of the continuous phase and the latent heat of the dispersed phase, respectively. The continuous phase Reynolds number at the orifice plate exit (Re_{co}) is:

$$\mathrm{Re}_{co} = \frac{4\rho_c \dot{m}_d D_{do}}{\pi\rho_{dl}\mu_c D_{or}^2 N_{or}} = \frac{4\rho_p \dot{m}_r D_{do}}{\pi\rho_{rl}\mu_p D_{or}^2 N_{or}} \tag{9}$$

The total dispersed mass flowrate ($\dot{m}_d$), the diameter of the orifice (D_{or}), and the number of orifices (N_{or}) were used to calculate the initial velocity of the exiting droplet. The Re_{co} is based on the initial droplet diameter (D_{do}). The rightmost side of Eq. (9) expresses Re_{co} in terms of the PCM and refrigerant properties, where the PCM and the refrigerant are the continuous and the dispersed phase, respectively.

Figure 3 shows the heat transfer measurements that Smith et al. (1982) made to determine the leading constant-γ and the exponent-x in eqs. (7) and (8). The measured superheat between the dispersed phase (cyclopentane) and the continuous phase (water) is plotted against the height of water required for complete evaporation. The circles and squares represent measurements for Re_{co} of 8880 and 13324, respectively. The first data set (Re_{co} = 8880) had 7 orifice holes spaced at 100 orifice diameters, while the second (Re_{co} = 13324) were done for 19 orifice holes spaced at 58 orifice diameters. The Re_{co} was calculated with an orifice diameter (D_{or}) of 0.5 mm and the D_{do} that was observed by Smith et al. (1982) in their experiments: 1 mm. For a fixed L, Smith et al. (1982) determined the required superheat for complete evaporation by reducing the superheat until cyclopentane began to appear as a layer on top of the water. From these measurements, Smith et al. (1982) provided 24 different regression constant sets for γ and x. For a given Re, the 24 sets of constants can produce greater than two orders of magnitude variation in the droplet heat transfer coefficient. Obviously, the provided constants cannot be used to design a DCHEX because it is not known which constants are valid. Consequently, the Smith et al. (1982) measurements were re-regressed in this study to provide a single value for γ and x for the observed droplet diameter of 1 mm. The single fit ($\gamma = 0.020 \pm 0.002$ and $x = 0.728 \pm 0.008$)[1] is shown to predict

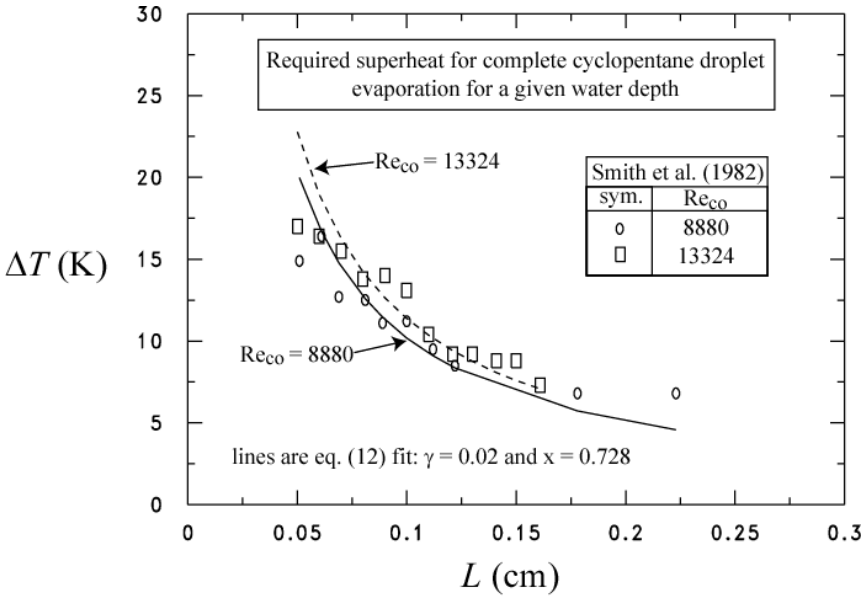

Figure 3 Required superheat for complete cyclopentane droplet evaporation for a given water depth (measurements from Smith et al. (1982))

[1] Uncertainties are for a 95 % confidence level.

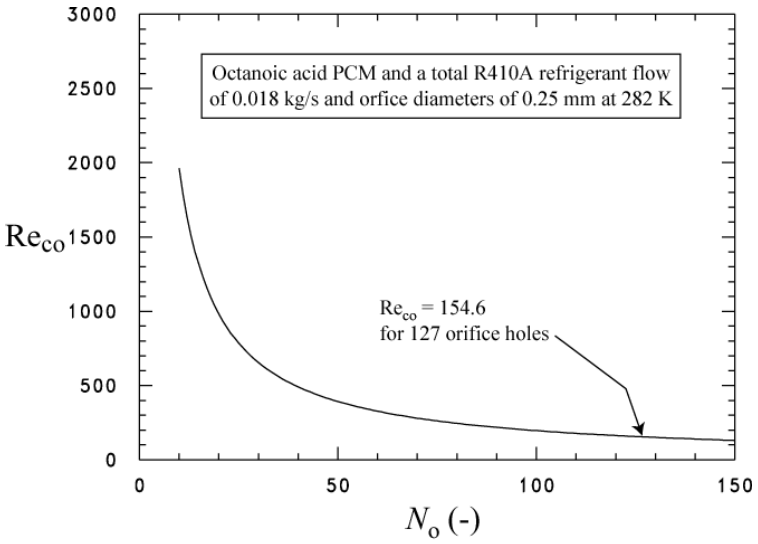

Figure 4 Refrigerant Reynolds number as a function of the number of orifices

approximately 77 % of the required continuous phase heights to within 0.14 mm for both Reynolds numbers as shown by the solid and dashed lines in Figure 3.

The justification for disregarding the fitting solutions of Smith et al. (1982) is mainly that their fits were obtained without varying the Re_{co}. This flawed methodology effectively treats the solution for the Re-exponent as a constant multiplier on γ. Statistical analysis requires that a parameter must be varied in order to determine its dependence on the data. In other words, the Re must be varied in order to regress the exponent on Re. Smith et al. (1982) did not do this. Instead, they regressed the two data sets for different Re as separate data sets, thus, losing the influence of Re. The fit provided here regresses the two data sets for the two different Re together in order to fit the value of x. The reason that Smith et al. (1982) gave for separating the data into two separate sets is that they claimed that the droplets agglomerated in one data set and not in the other. They provided no evidence for agglomeration or lack of agglomeration except for a flawed argument that the void fraction was larger for the larger Re data set. The void fraction was greater because, for a fixed continuous-phase mass, when the dispersed phase mass flowrate is increased via increased Re, by definition, the void fraction must increase. For the Smith et al. (1982) experimental configuration, the void fraction increased for increased Re independent of droplet/bubble agglomeration. Further justification for ignoring the claimed effect of agglomeration is that the Smith et al. (1982) derived solution for agglomeration differs mainly from their pre-agglomeration derivation by the exponent on the droplet velocity, which contains the exponent-x. If the derivation distinguishes between agglomeration and pre-agglomeration stages with a different exponent, but the present regression fits both data sets well with a single exponent, then this suggests that agglomeration is not significant. Finally, it is not clear how 19 orifice holes, with a spacing that is 58 orifice diameters, will produce significantly more agglomeration than 7 orifice holes with a spacing that is 100 orifice diameters.

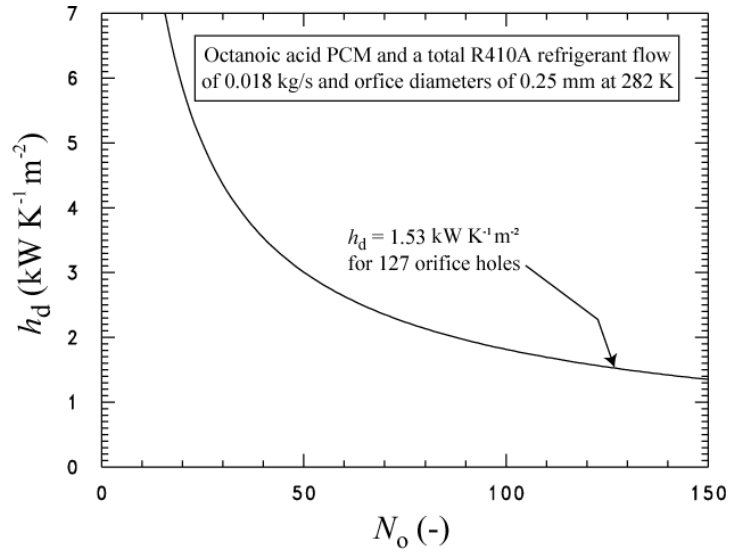

Figure 5 Droplet heat transfer coefficient as a function of the number of orifices

Figure 4 plots the refrigerant droplet Reynolds number evaluated at the nozzle (Re_{co}), given in Eq. (9), as a function of the number of orifice holes. The Reynolds number is based on half of the refrigerant mass flow because it is divided between two identical DCHEXs. As will be illustrated, the 0.25 mm orifice diameter was chosen as a compromise to limit the height of the DCHEX by maintaining larger droplet heat transfer coefficients. For between ten and 150 orifice holes, the boundary layer on the spherical droplet is laminar because the Reynolds number is always less than 2×10^5 (Incropera and DeWitt, 2002). Smaller Reynolds numbers will lead to smaller droplet heat transfer coefficients according to Eq. (7) and shown in Figure 5. Figure 5 shows that the heat transfer coefficient varies by approximately 222 % from 50 to 10 orifice holes. While h_d changes by approximately 55 % from 50 to 150 orifice holes. Obviously,

the droplet heat transfer is more sensitive to the number of orifice holes chosen for designs with less than 50 orifice holes than it is for designs with more than 50 orifice holes.

Figure 6 shows the height (L) of the PCM column required to completely evaporate an all-liquid refrigerant droplet to saturated vapor. Eq. (8) was used to solve for L while using the properties of the refrigerant and the PCM that are given in Table 1 (Kedzierski and Lin, 2020). In addition, a superheat of 8 K, a total refrigerant flowrate of 0.018 kg/s, and the regression constants as determined in the present analysis ($\gamma = 0.02$ and x = 0.728) were used. Results for three different orifice diameters are shown. The solid line shows the predictions using an orifice diameter and the droplet diameter of 0.25 mm and 0.50 mm, respectively. Two dashed lines above and below the solid line show predictions using orifice diameters of 0.50 mm and 0.10 mm, respectively. In general, Figure 6 shows that the required PCM column height decreases as the number of orifice holes increases and as the orifice diameter decreases. If maximizing the droplet heat transfer shown in Figure 5 was the only design consideration, then the DCHEX would be designed with 10 orifice holes or less and with the 0. 5 mm orifice diameter. As Figure 6 shows, the design that uses ten 0.5 mm diameter orifice holes requires a PCM height of nearly 2.2 m, which closely approaches the ceiling height of most residential basements. To remain within the vertical space limitations of most residential basements, the PCM column height (L) must reside within the shaded region of Figure 6. i.e. $L < 1.2$ m. Consequently, a design using 0.50 mm diameter orifice holes is not possible if N_{or} is to be limited to 150 because all required PCM heights are greater than 1.2 m. Conversely, Figure 6 shows that all of the designs using the 0.10 mm diameter orifice holes result in acceptable PCM column heights. However, it was felt that the 0.10 mm orifice was more likely to be out of the range of validity for the droplet heat transfer correlation than the predictions for the 0.25 mm diameter design. For this reason, the 0.25 mm orifice hole design was chosen near the allowable limit for L. This design gave 127 orifice holes (0.25 mm diameter) and a column height of 1.08 m.

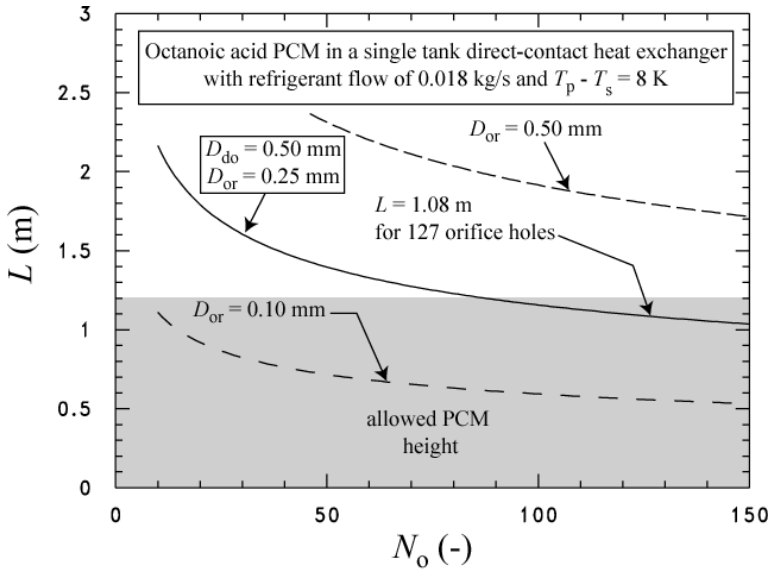

Figure 6 Height of PCM column in direct-contact heat exchanger

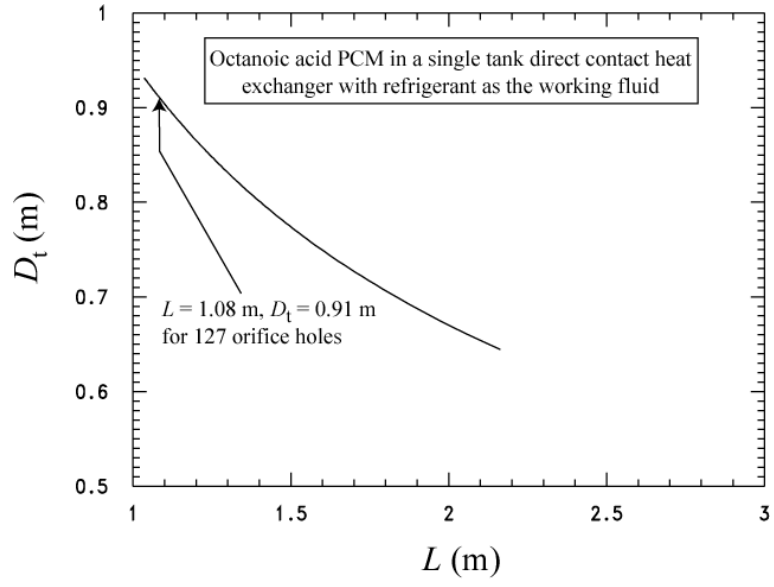

Figure 7 Diameter of direct-contact heat exchanger and a function of tank height

Figure 7 shows that, given the constraint of fixed PCM mass, the required diameter of the heat exchanger (D_t) is 0.91 m for L = 1.2 m. Spotts et al. (2004) give the pressure vessel wall thickness (t) necessary to resist a yield stress (S) due to a design pressure (P):

$$t = \frac{PD_t / 2}{S - 0.6P} + t_c = 13\text{mm} + 2\text{mm} = 15\text{mm} \tag{10}$$

The allowed yield stress used in Eq. (10) for A-106-GR.B steel was 175.2 N/mm^2 (Spotts et al., 2004). The t_c is the thickness to allow for corrosion of the steel over time. A design pressure of 5 MPa was used considering that the pressure of R410A should always remain less than 4 MPa (Prah, 2001). Considering the length, diameter and thickness, end caps, the mass of each heat exchanger without PCM is approximately 400 kg. The mass of each DCHEX, including the PCM, is approximately 1043 kg. The total mass of each DCHEX will be slightly larger than 1043 kg when the mass of the ancillary equipment, such as support legs, piping, and orifice plate, is included.

3. FUTURE WORK

An accurate transient pressure drop model needs to be developed for a dispersed phase flowing through a continuous freezing phase. In addition, the Smith et al. (1982) model needs to be improved with more data for more fluids, operating conditions, and orifice diameters. This will allow the optimization of the DCHEX for maximum heat transfer and minimum pressure drop. In general, comprehensive investigations are needed to understand the fundamentals and to develop simulation tools that can be used to design PCM-DCHEXs for different thermal energy applications. This would involve the search for new PCMs. Machine-learning-assisted screening could be an efficient tool to search for optimal phase change materials to be used for energy storage. Finally, the heat exchanger designed here needs to be constructed, installed and tested in the NZERTF.

4. CONCLUSIONS

A viable thermal energy storage (TES) design for a residential air-conditioner hinges on reducing the thermal resistances associated with charging and discharging a phase change material (PCM). Direct contact heat exchange between the PCM and the heat-pump refrigerant of is one approach toward significantly reducing thermal resistances and improving the efficiency of residential TES. Direct-contact heat exchange eliminates physical barriers that significantly contribute to the heat transfer resistance between the refrigerant and the PCM. As a necessary step prior to testing residential TES, a direct-contact heat exchanger was designed and sized for the National Institute of Standards and Technology's Net-Zero Energy Residential Test Facility (NZERTF).

For the heat exchanger design, octanoic acid was chosen as the PCM and R410A as the refrigerant because these fluids are immiscible with each other and less likely to supercool. Twin heat exchangers were designed to house a vertical column of PCM and to distribute the refrigerant flow throughout the PCM. A key design parameter was the height of the PCM column. The PCM height had to be tall enough to completely evaporate a liquid refrigerant droplet and short enough to fit within the vertical space limitations of a typical residential basement. This height was found to be 1.2 m, which fixed the diameter at 0.91 m. The mass of each heat exchanger is approximately 1043 kg. Measurements from the literature were re-correlated to predict the droplet heat transfer coefficient and the required height of the PCM column. A disengagement section was designed to prevent entrainment of PCM droplets into the exiting refrigerant vapor during the PCM charging. Basic equations are provided so that the design may be modified for different a PCM mass, refrigerant flow rate, temperature difference and operating fluids. An overall drawing of the heat exchanger with placement of orifice holes is given. The energy storage capacity of the DCHEX is approximately 191 MJ and has the potential of providing a 33 % energy savings in cooling the NZERTF.

NOMENCLATURE

English symbols		**Greek symbols**	
C_d	drag coefficient (-)	ΔT	temperature difference between continuous and dispersed phases (K)

D	diameter (m)	γ	dimensionless fitted constant in eqs. (7) and (8)
F_b	buoyance force (N)	λ_p	latent heat of melting ($J \cdot kg^{-1}$)
F_d	drag force (N)	μ	dynamic viscosity ($kg \cdot m^{-1} \cdot s^{-1}$)
F_g	gravity force (N)	ρ	density ($kg \cdot m^{-3}$)
g	gravitational acceleration constant ($m \cdot s^{-2}$)	σ	surface tension ($N \cdot m^{-1}$)
h_d	droplet heat transfer coefficient ($W \cdot m^{-2} \cdot K^{-1}$)	ΔT	temperature difference between continuous and dispersed phases (K)
H_D	disengagement height (m)	γ	dimensionless fitted constant in eqs. (7) and (8)
i_{fg}	latent heat of vaporization ($kJ \cdot kg^{-1}$)		
i_{fs}	heat of fusion ($kJ \cdot kg^{-1}$)		
k	thermal conductivity ($W \cdot m^{-1} \cdot K^{-1}$)		

Subscripts

c	continuous phase
co	continuous phase evaluated at orifice
d	dispersed phase or droplet
do	droplet at orifice
dl	dispersed phase liquid
dv	dispersed phase vapor
l	liquid
m	melting
p	phase change material
rl	refrigerant liquid
rv	refrigerant vapor
t	heat exchanger tank
v	vapor

REFERENCES

Baxter, V.D., and Moyers, J.C. 1985. Field-measured cycling, frosting, and defrosting losses for a high-efficiency air-source heat pump. ASHRAE Trans. Vol. 91:2B. 537-554.

Clift, R., Grace, J.R.,Weber, M.E. 1978. Bubbles, Drops, and Particles, Academic Press, New York, NY.

Deepu, P., Basu, S., 2014. Effect of evaporation and agglomeration on droplet shape oscillations. Chem. Eng. Sci. 119, 212–217. https://doi.org/10.1016/j.ces.2014.08.033

GPSA. 2004. Engineering Data Book, Gas Processors Suppliers Association (GPSA), 12th ed, Tulsa, OK, p. 7-11.

Incropera, F. P., and DeWitt, D. P. 2002. Fundamentals of Heat and Mass Transfer, 5th ed., John Wiley & Sons, New York.

Kedzierski, M. A., and Lin, L. 2020. Design of a Direct-Contact Thermal Energy Storage Heat Exchanger for the NIST Net-Zero Residential Test Facility, NIST Technical Note 2104, U.S. Department of Commerce, Washington, D.C.

Kedzierski, M. A., Payne, W. V., and Skye, H. M. 2018. Thermal Energy Storage for the NIST Net-Zero House Heat Pump, NIST Technical Note 2005, U.S. Department of Commerce, Washington, D.C.

Kedzierski, M. A., Payne, W. V., and Skye, H. M. 2014. Potential Research Areas in Residential Energy Storage for NIST's Engineering Laboratory, NIST Technical Note 1844, U.S. Department of Commerce, Washington, D.C.

Prah, F. 2001. Refrigerant 410A, Refrigeration Service Engineers Society, Des Plaines, Illinois, 620-108 Section 3, https://www.rses.org/assets/r410a/R-410A.PDF

Sideman, S., Gat, Y. 1966. Direct contact heat transfer with change of phase: Spray-column studies of a three-phase heat exchanger. AIChE J. 12, 296–303. https://doi.org/10.1002/aic.690120217

Smith, R.C., Rohsenow, W.M., Kazimi, M.S. 1982. Volumetric Heat-Transfer Coefficients for Direct-Contact Evaporation. J. Heat Transfer 104, 264–270. https://doi.org/10.1115/1.3245082

Spotts, M.F., Shoup, T.E., Hornberger, L.E. 2004. Design of Machine Elements, Prentice Hall. 8th ed.

ACKNOWLEDGEMENT

This work was funded by Exploratory Research Project of the National Institute of Standards and Technology (NIST). Thanks go to Dr. Riccardo Brignoli and to Dr. W. Vance Payne of NIST for their constructive criticism of the draft manuscript.